Middle Eocene to early Oligocene calcareous nannofossil biostratigraphy at IODP Site U1333 (equatorial Pacific)

Federica Toffanin[1], Claudia Agnini[1,2], Domenico Rio[1], Gary Acton[3], Thomas Westerhold[4]

[1]Dipartimento di Geoscienze, Università di Padova,
Via Giovanni Gradenigo, 6, I-35131 Padova, Italy
[2]Istituto di Geoscienze e Georisorse, CNR-Padova c/o Dipartimento di Geoscienze,
Università di Padova, Via Giovanni Gradenigo, 6, I-35131 Padova, Italy
[3]Department of Geology, University of California, Davis,
One Shields Avenue, Davis, 95616, CA, USA
[4]MARUM — Center for Marine Environmental Sciences, University of Bremen,
Leobener Strasse, 28359 Bremen, Germany
corresponding author: claudia.agnini@unipd.it

ABSTRACT We present a biostratigraphic and biochronologic study of calcareous nannofossils of middle Eocene - early Oligocene age recovered during IODP Expedition 320, at Hole U1333C in the equatorial Pacific Ocean. The study succession encompasses nannofossil Zones NP16–NP21 (equivalent to CP13–CP16) and Chrons C20r–C12r (middle Eocene-early Oligocene). The distribution patterns of calcareous nannofossil taxa are studied by means of relative abundance and semiquantitative counts with the final aim to test the reliability of biohorizons used in the Paleogene standard biozonations (Martini 1971; Okada and Bukry 1980) and check alternative bioevents included in a more recent mid-latitudes biostratigraphic scheme (Fornaciari et al. 2010). Calibration ages are estimated based on the ranges of the biozones relative to a detailed magnetostratigraphy constructed for the site. Of particular biostratigraphic significance, our study shows that the Top of *Sphenolithus furcatolithoides*, the Base of common and continuous occurrence (Bc) of *Dictyococcites bisectus* and the total range of *Sphenolithus obtusus* can be used to better constrain the middle Eocene interval. The studied sediments cover the crucial time period that followed maximum Cenozoic warmth and led up to the initial major glaciation on Antarctica, including two important climatic events, the Middle Eocene Climatic Optimum (MECO), a transient episode of global warming during a long-term cooling trend, and the Oi-1 event. The peculiar regime in sedimentation observed in the equatorial Pacific, which roughly consists of alternating phases of Carbonate Accumulation Events (CAE) and crashes in carbonate content, are correlated with increases and decreases in calcareous nannofossil abundances. A more detailed comparison indicates that the MECO corresponds to an interval with very low carbonate in between CAE3 and CAE4. This event is correlative with the Top of *S. furcatolithoides*, the Bc of *D. bisectus* and a prominent increase in the relative abundance of heavy calcified nannofossils (e.g., discoasters).

Key words: calcareous nannofossils, biostratigraphy, middle Eocene/early Oligocene, equatorial Pacific

INTRODUCTION

The Eocene time was an intriguing interval because it represents the transition between Greenhouse climatic conditions, that lasted through the Eocene, climaxing in the early Eocene climatic optimum (EECO; ca. 50 Ma), and Icehouse conditions (Zachos et al., 2001; 2008), initiated at the base of the Oligocene ca. 33.8 Ma, with the O-1 event and correlated with the onset of large icesheets in the southern hemisphere (Miller et al. 1991; Zachos et al 1992). The long-term cooling trend initiated after the EECO was not monotonic, but instead was punctuated by several transient cooling and warming episodes (Bohaty and Zachos 2003; Edgar et al. 2007; Sexton et al. 2006; 2011; Tripati et al. 2005a; Westerhold and Röhl 2009).

The early Eocene was a time of extremely warm climates, reaching the warmest temperature of the past 80 Myr, but also of progressive deterioration, during the middle to late Eocene, coinciding with permanent changes in calcareous plankton (Aubry 1992; 1998; Wade 2004; Aubry and Bord 2009). Unfortunately, calcareous nannofossils from this period are poorly documented in expanded and/or well-preserved stratigraphic successions (Fornaciari et al. 2010) and this lack is particularly evident in the material recovered from the equatorial Pacific Ocean (ODP Leg 199; text-fig. 1), where middle to upper Eocene sediments can be broadly described as radiolarian ooze and clay (Lyle and Wilson 2006). The Pacific Equatorial Age Transect (PEAT) program conducted during IODP Expeditions 320 and 321, recovered a continuous record of this interval, which indicated the calcium carbonate depth (CCD) was very dynamic and shallow during the Eocene, with numerous excursions of as much as 500m (Lyle et al. 2010; Pälike et al. 2010; 2012). The recovered drill cores represent an exceptional archive in which modifications of nannoplankton assemblages can be thoroughly investigated in the equatorial Pacific (Bown and Dunkley Jones 2012). Relative abundance and semiquantitative counts of calcareous nannofossils were performed for the middle Eocene to early Oligocene interval with the two-fold aim to provide a robust biostratigraphic framework and investigate causes of environmental-forced change in nannoplankton assemblages.

MATERIALS AND METHODS

Materials

IODP Site U1333 is located in the equatorial Pacific (12°04.0892'N, 142°09.720'W; 5113 mbsl; text-fig. 1) and represents the third oldest and deepest component of the PEAT depth transect. At Site U1333, seafloor basalt is overlain by ca. 183 m of pelagic sediment, dominated by nannofossil and radiolarian ooze with varying amounts of clay (Expedition 320/321 Scientists 2010; Pälike et al. 2010). Three holes were cored at the site allowing a complete

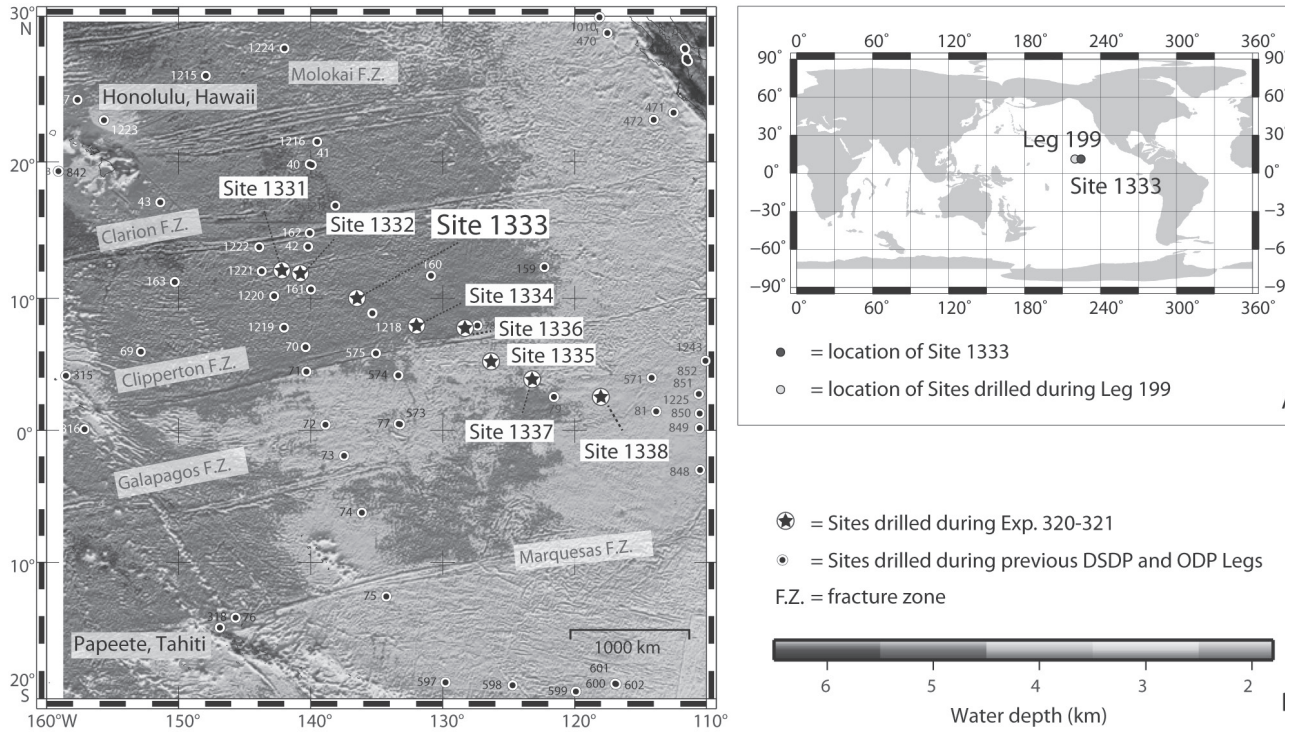

TEXT-FIGURE 1
A) Locations of IODP Leg 199 drilling sites and IODP Site 1333 (http://www.odsn.de/odsn/services/paleomap/paleomap.html); B) Detailed location map of sites drilled during Exp. 320-321, previous DSDP and ODP sites are also reported (modified after Pälike et al., 2009).

composite section to be constructed with minimal stratigraphic gaps (Expedition 320/321 Scientists 2010; Westerhold et al. 2012). Depths below seafloor for this composite section are given in a "adjusted revised meters composite depth" (armcd) scale as described by Westerhold et al. (2012). The armcd mapping procedure allows data and samples located outside the spliced composite record to be placed in the new revised composite depth scale at each hole and site. We focus our sampling on sediments from 192.06 to 124.80 armcd in Hole 1333C, with samples collected every 20 to 40 cm in the interval from 178 to 159 armcd and about every 100 cm in the basal and upper parts of the section. The study material consists of biogenic sediments comprising clayey nannofossil ooze, nannofossil radiolarian ooze, nannofossil ooze, radiolarian nannofossil ooze, and porcellanite in the middle to upper Eocene, and alternating very pale brown nannofossil ooze and yellowish brown nannofossil ooze with radiolarians in the upper Eocene-lower Oligocene. Mean accumulation rates are about 4-5 m/Myr from 45 to 31 Ma (middle Eocene to early Oligocene) and increase up to ca. 12 m/Myr from the early Oligocene. In the Eocene, $CaCO_3$ contents vary abruptly between <1 and 74 wt% because of variations of equatorial Pacific CCD (Pälike et al. 2012). The Eocene paleodepth for IODP Site U1333 is estimated to have been ca. 3800m and preliminary results reported sediments with high carbonate content around the MECO event, providing the opportunity to study the high-carbonate preservation events (CAEs) in relation to global modification in Earth's climate (Lyle et al. 2005; Pälike et al. 2010).

METHODS

Calcareous Nannofossils

We prepared 109 smear-slide samples for calcareous nannofossil analysis from unprocessed material using standard techniques described in Bown and Young (1998). Smear slides were then analyzed with a Zeiss Axiophot optical microscope, at 1250X magnification. Calcareous nannofossils were determined using the taxonomy of Perch-Nielsen (1985) and Aubry (1984; 1988; 1989; 1990; 1999), except for sphenoliths for which we have followed Fornaciari et al. (2010). The biostratigraphic standard schemes of Martini (1971) and Okada and Bukry (1980) were applied and compared with the mid latitude zonal scheme recently published by Fornaciari et al. (2010). Age calibration of calcareous nannofossil biohorizons is based on magnetostratigraphic data available for Site U1333.

The state of preservation, the degree of dissolution and/or overgrowth of calcareous nannofossil assemblages vary throughout the study interval. We thus decided to describe every sample following the qualitative classification proposed by Roth and Thierstein (1972) and Roth (1983). This approach provides three main subgroups of samples, that are defined as follows: 1) well preserved (G) for samples with slightly etched and/or overgrown coccoliths; 2) moderately preserved (M) for samples with moderate etching and/or overgrowth, 3) poorly preserved (P) for strongly etched and/or overgrown coccoliths assemblages with reduced diversity. Additionally a specific classification for etching and overgrowth is also provided (see Table 1 supplementary data).

Relative abundance analyses, expressed in percentage, were estimated for species and genera based on counts of at least 300 specimens. Semiquantitative data are determined counting all calcareous nannofossil specimens present in a prefixed area (1 mm^2, 50 fields of view). To monitor the species abundance within the same genus, a total of 100 specimens belonging to *Discoaster* and *Sphenolithus* were counted following the strategy of Rio et al. (1990). To provide a more reliable biostratigraphic framework,

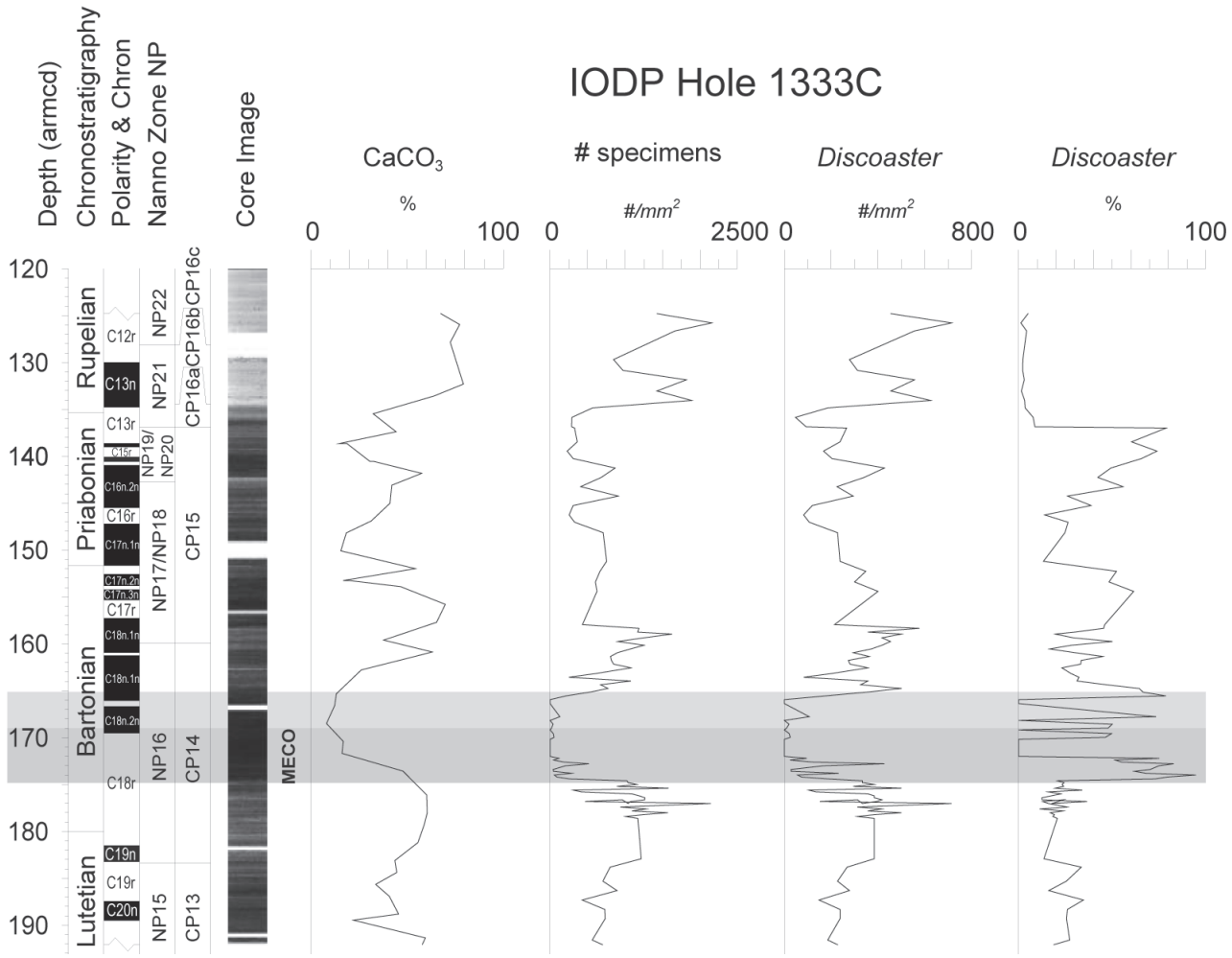

TEXT-FIGURE 2
Abundance patterns of *Discoaster*, total number of specimens in a prefixed area (#/mm2) and $CaCO_3$ content (after Pälike et al. 2010) from the IODP Hole 1333C are plotted against magnetostratigraphy and biostratigraphy (NP—Martini, 1971; Okada and Bukry 1980). The light grey shaded bar emphasizes the MECO event that correlates with one of the episodes of CCD shallowing during the Eocene. Chronostratigraphic boundaries are located following the Geological Time Scale 2012 (GTS2012; Gradstein et al. 2012).

additional counts were carried out in a prefixed area of 9 mm^2 (three transects) for *Chiasmolithus solitus, C. grandis, C. oamaruensis* and *Isthmolithus recurvus*, which are index species that are very rare to virtually missing in the study material.

Magnetostratigraphy and age model

Cleaned paleomagnetic data provide a series of distinct ~180° alternations in declination and subtle changes in inclination, which, when combined with biostratigraphic age constraints, allow a continuous magnetostratigraphy to be constructed that correlates well with the geomagnetic polarity timescale (Expedition 320/321 Scientists 2010; Pälike et al. 2010; Acton et al., unpublished data). In Table 1, we report ages and relative positions of bioevents in relation to magnetochrons based on the GPTS of Cande and Kent (1995; CK95).

The MECO event is here tentatively correlated with the low carbonate content interval observed from ca. 174 to 166 armcd, which is associated with a clear decrease in calcareous nannofossil abundance. In particular, the onset of the MECO event is placed ca. 500 kyr before the base of Chron C18r following Bohaty et al. (2009).

RESULTS AND DISCUSSION

Calcareous nannofossils are present and moderately to poorly preserved through most of the study material with some short barren/very impoverished intervals in the middle/upper Eocene. The study interval spans a complete sequence of nannofossil zones from middle Eocene Zone NP15 to lower Oligocene Zone NP22 in which fossil assemblages are mainly composed of discoasters, placoliths and sphenoliths. The relative abundance of *Discoaster* and *Sphenolithus* is highly variable and anti-covariant. Placoliths are well represented in the assemblages with *Dictyococcites* showing a relative abundance pattern similar to that of *Discoaster* and opposite to the other placoliths (*Reticulofenestra, Coccolithus, Ericsonia*).

Dissolution and preservation

The preservation of carbonate microfossils is mainly affected by primary and export productivity as well as by water-column and seafloor chemistry. In particular, at Site U1333, the strength of dissolution is directly related to the depth/paleodepth and fluctuations of the CCD of the drilling site (Pälike et al. 2010; 2012; Bown and Dunkley Jones 2012). Estimates of Eocene equatorial CCD give depths that are shallower than 3.5 km (Lyle

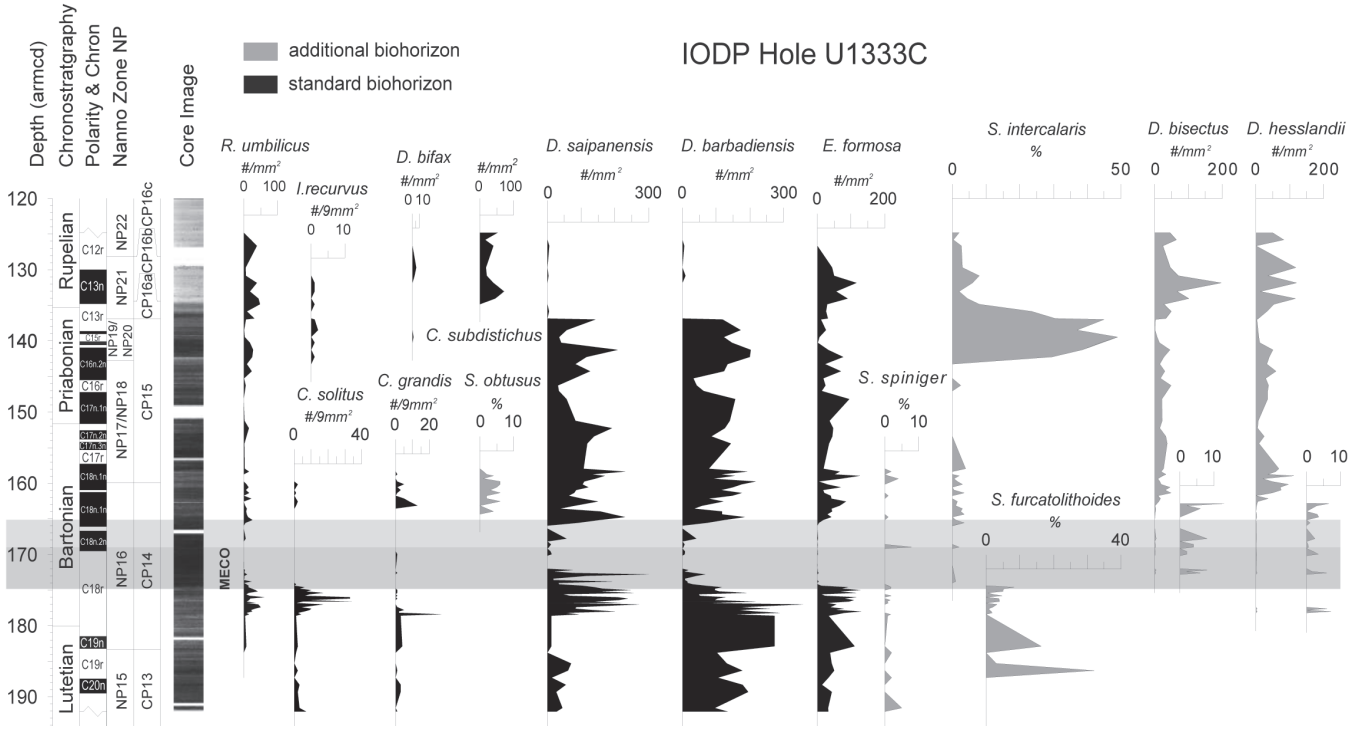

TEXT-FIGURE 3
Abundance patterns of standard and additional calcareous nannofossil index taxa from the IODP Hole 1333C are plotted against magnetostratigraphy and biostratigraphy (NP—Martini 1971; Okada and Bukry 1980). The light grey shaded bar emphasizes the MECO event that correlates with one of the episodes of CCD shallowing during the Eocene. Chronostratigraphic boundaries are located following the Geological Time Scale 2012 (GTS2012; Gradstein et al. 2012).

et al. 2005), with several CCD shallowing phases occurring during the middle to late Eocene. However, the most striking change in carbonate sedimentation is the CCD deepening at the Eocene–Oligocene transition, which produces a shift from siliceous sediments to calcareous plankton oozes (Pälike et al. 2010).

Overall, coccoliths are found to be more abundant than foraminifera close to CCD (e.g.; Hay 1970; McIntyre and McIntyre 1971) and are often present even in very low carbonate sediments. Within the nannofossil assemblages, however, certain taxa are more resistant than others to dissolution and their abundance can be investigated with the aim of reconstructing the degree of dissolution through time (Henriksen et al. 2004; Hassenkam et al. 2011; Toffanin et al 2011). At Hole U1333C, the preservation of the calcareous nannofossil assemblages varies throughout the study succession, from moderate to poor. In particular, 13 barren samples are found during the MECO (ca. 172-170 armcd). In the same interval, between 174.40 and 165.15 armcd, an overall decrease in preservation is observed with samples showing strong dissolution. In general, calcareous nannofossil assemblages are strongly affected by dissolution, ranging from moderate (etching level E-2) below and above the critical interval to strong (etching level E-3) during the event.

The degree of preservation of an assemblage is affected by two main factors, calcite overgrowth and dissolution (Roth and Thiestein 1972; Roth 1983). In our samples, overgrowth processes are sporadically occurring only in large specimens of heavily-calcified genera, for instance, *Discoaster, Reticulofenestra* and *Dictyococcites*. In general, overgrowth blurs species specific features making correct identification of species difficult. The overgrowth process is thus able to modify the relative abundance of some taxa within the assemblage, because of incorrect identification, but does not significantly alter the absolute abundance of calcareous nannofossil taxa. On the contrary, dissolution, which is by far the most common process affecting calcareous nannofossil assemblages in our material, is species preferential and therefore alters both the relative and absolute abundance of calcareous nannofossil taxa (Roth and Thierstein 1972). The way by which dissolution modifies calcareous nannofossil assemblages is twofold. Firstly, it lowers the total number of taxa observed (species richness), dissolving the more fragile species almost completely. This mechanism eventually results in higher relative abundances of dissolution-resistant taxa and lower relative abundance or even absence of more delicate species (Bornemann and Mutterlose 2008). Secondly, it causes the decrease of absolute abundance of calcareous nannofossils taxa, even the more resistant and robust ones. The stronger the dissolution, the lower the number of specimens in a prefixed area.

Looking back over our data, if dissolution would have severely affected nannofossil taxa, the assemblage should be dominated by dissolution-resistant taxa, such as *Discoaster* (Adelseck et al. 1973). The absolute and relative abundance patterns of discoasters are thus used to evaluate the degree of dissolution. Actually, this genus shows a prominent decrease in the number of specimens present in a prefixed area (mm^2). Indeed a remarkable increase in the relative abundance of discoasters was also observed. These two abundance patterns, that seem apparently irreconcilable, are on the contrary easily explained if we consider the fossil calcareous nannofossil assemblage as the result of a pristine assemblage altered/biased by preferential dissolution, where even the most resistant taxa decrease in absolute abundance,

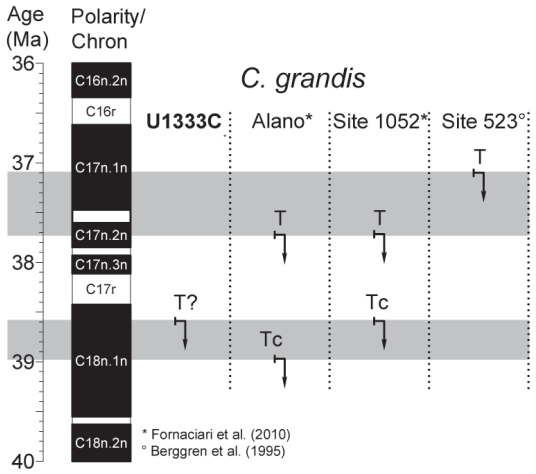

TEXT-FIGURE 4
Age estimates for the Top common and Top of C. grandis. The GPTS used to calibrate this biohorizon is that of CK95 (see also Table 1).

but obviously increase their relative abundance becoming the dominant taxa in dissolved assemblages.

Changes in the absolute and relative abundance of calcareous nannofossils observed during the MECO are correlated with an episode of CCD shallowing (text-fig. 2; Bohaty et al. 2009; Pälike et al. 2010). Very similar modifications are found to recur at least two more times before the end of the Eocene virtually mirroring $CaCO_3$ contents and CCD reconstruction. At the base of the Rupelian, a final increase in the absolute abundance of calcareous nannofossils is associated with a prolonged increase in carbonate content suggesting a permanent deepening of the equatorial Pacific CCD (text-fig. 2; Pälike et al. 2010; 2012).

Calcareous nannofossil biostratigraphy

Calcareous nannoplankton first appeared in the Late Triassic as low diversity assemblages and rapidly radiated during the Early Jurassic (Bown et al. 2004). From that time they have colonized the oceans and their abundance, wide geographic distribution and rapid evolution have been used in biostratigraphy. In fact, the stratigraphic distributions of calcareous nannofossil taxa are utilized to construct a number of standard biozonations. For the Paleogene interval these biostratigraphic frameworks have been assembled by Martini (1971) and Okada and Bukry (1980), but more recently, other authors (i.e.; Catanzariti et al. 1997; Fornaciari et al. 2010) have proposed new biostratigraphic schemes for the middle Eocene-early Oligocene interval.

Here, we identified the biohorizons of the Paleogene standard zonations of Martini (NP; Martini 1971) and Okada and Bukry (CP; Okada and Bukry 1980), as well as those of the mid latitude biostratigraphic zonal scheme of Catanzariti et al. (1997), integrated by Fornaciari et al. (2010). The following biohorizons were used: Base (B), Base common (Bc), Top common (Tc), Top (T) and Cross-over (X) following Backman et al. (2012).. Additionally, we used two types of biohorizons based on intervals in which the abundance of a certain taxon is significantly more abundant than in the rest the stratigraphic record (acme interval). We thus refer to as the Base of increased abundance (Bi) where a notable increase in abundance of a certain taxon is observed, while we define the Top of increased abundance (Ti) where the same taxon shows a remarkable decrease in abundance.

Abundance patterns of the index species adopted in considered zonal schemes are reported in text-figure 3. Images of the standard markers and several other calcareous nannofossil taxa are provided in Plates 1-2. The taxonomic list of taxa observed during this study is available in Appendix 1.

Standard calcareous nannofossil biohorizons

The Base of *Reticulofenestra umbilicus*

The Base of *R. umbilicus* defines the base of CP14a Zone of Okada and Bukry (1980) and is used to approximate the base of NP16 Zone of Martini (1971) when *Blackites gladius* is missing (Perch-Nielsen 1985). At Hole 1333C the Base of *R. umbilicus* >14µm occurs within Chron C19r (184.55 ± 0.75 armcd; Table 1), consistent with previous findings (Wei and Wise; 1989; Jovane et al. 2007; Fornaciari et al. 2010). The taxonomic concept of *R. umbilicus* proposed by Backman and Hermelin (1986), which includes all specimens >14µm, is now commonly accepted and the more recent calibrations based on this morphometric definition seem to minimize the large discrepancies existing in previous age estimations.

The Top of *Blackites gladius*

The Top of the *B. gladius* defines the base of NP16 Zone of Martini (1971). This species is very fragile and tends not to be preserved in deep-sea sediments (e.g. Bukry et al. 1971; Backman 1986) and is seldom reported from deep-sea settings (Wei and Wise 1989). Here, the species is absent likely because of the poor preservation, thus preventing its use for biostratigraphic aims.

The Top of *Chiasmolithus solitus*

The Top of *Chiasmolithus solitus* defines the base of Zones NP17 and CP14b (Martini 1971; Okada and Bukry 1980). The species is reported to be scarce in low latitude sediments and diachronous at different latitudes (Perch-Nielsen 1985; Wei and Wise 1992; Aubry 1992; Villa et al. 2008; Fornaciari et al. 2010). At Hole 1333C, *C. solitus* is present but very rare up to ca. 160 armcd (159.95 ± 0.20; Table 1), in the upper part of Chron C18n.1n. This datum is quite consistent with recent findings from mid-high latitudes (Villa et al. 2008; Fornaciari et al. 2010) but some previous studies reported a final extinction of this taxon in Chron C18r in low-mid latitude areas (Poore et al. 1984; Wei and Wise 1989; 1990a).

The Top of *Discoaster bifax*

The Top of *D. bifax* is used by Okada and Bukry (1980) to mark the base of CP14b Zone. This species is usually common in equatorial sediments (e.g., Bukry 1973) and rare/absent at middle to high latitudes (Percival 1984; Proto Decima et al. 1975; Nocchi et al. 1988; Wei and Wise 1989; 1992; Wei and Thierstein 1991; Marino and Flores 2002a; b; Fornaciari et al. 2010). At Hole 1333C, only few specimens of *D. bifax* were observed during the analysis within CP16 Zone, a more continuous presence has been reported by Bown and Dunkley Jones (2012). The Top of *D. bifax* is not used in this study.

The Base of *Chiasmolithus oamaruensis*

The Base of this species defines the base of NP18 Zone and is secondarily used to define the CP15a Zone as a secondary biohorizon (Martini 1971; Okada and Bukry 1980). Previous authors reported a rare presence of *C. oamaruensis* from low latitude areas (e.g., Wei and Wise 1989). These data are confirmed by the absence of this taxon at Site 1333 and, overall, in equatorial Pacific sites (U1331-U1334; Bown and Dunkley Jones 2012).

TABLE 1
The positions of biohorizons are reported together with their chron notations and age estimations.

Type of event	Species	Sample Base	Int (cm)	Sample Top	Int (cm)	Depth Base (mbsf)	Depth Top (mbsf)	Depth Base (rmcd)	Depth Top (rmcd)	Depth Base (armcd)	Depth Top (armcd)	Average Depth (armcd)	Depth Uncertainty (± m)	Chron Base*	Chron Top*	Age Base[1] (Ma)	Age Top[1] (Ma)	Average Age (Ma)	Age Uncertainty (± m)
T	*E. formosa*	U1333C-14H-1	135	U1333C-13H-7	70	108,950	107,800	130,850	126,800	130,850	126,639	128,745	2,106	C13n	C12r	33,320	32,944	33,132	0,188
Bi	*C. subdistichus*	U1333C-14H-5	35	U1333C-14H-4	85	113,950	112,950	135,850	134,850	135,850	134,850	135,350	0,500	C13r	C13n/C13r	34,093	33,720	33,906	0,186
T	*D. saipanensis*	U1333C-14H-5	135	U1333C-14H-5	35	114,950	113,950	136,850	135,850	136,850	135,850	136,350	0,500	C13r	C13r	34,466	34,093	34,279	0,186
Bc	*I. recurvus*	U1333C-15H-4	45	U1333C-15H-3	95	122,050	121,050	144,250	143,250	144,250	143,250	143,750	0,500	C16n.2n	C16n.2n	36,160	36,003	36,082	0,079
Ba	*S. intercalaris*	U1333C-15H-4	45	U1333C-15H-3	95	122,050	121,050	144,250	143,250	144,250	143,250	143,750	0,500	C16n.2n	C16n.2n	36,160	36,003	36,082	0,079
T	*S. obtusus*	U1333C-17H-2	5	U1333C-17H-1	115	132,650	132,250	158,350	157,950	158,350	157,950	158,150	0,200	C18n.1n	C18n.1n	38,587	38,537	38,562	0,025
T	*C. grandis*	U1333C-17H-2	45	U1333C-17H-2	5	133,050	132,650	158,750	158,350	158,750	158,350	158,550	0,200	C18n.1n	C18n.1n	38,637	38,587	38,612	0,025
T	*C. solitus*	U1333C-17H-3	35	U1333C-17H-2	145	134,450	134,500	160,150	159,750	160,150	159,750	159,950	0,200	C18n.1n	C18n.1n	38,813	38,763	38,788	0,025
B	*S. obtusus*	U1333C-17H-6	5	U1333C-17H-5	115	138,650	138,250	164,350	163,950	164,350	163,950	164,150	0,200	C18n.1n	C18n.1n	39,339	39,289	39,314	0,025
Bc	*D. hesslandii*	U1333C-18H-5	105	U1333C-18H-5	85	146,290	146,090	172,790	172,590	172,790	172,590	172,690	0,100	C18r	C18r	40,432	40,410	40,421	0,011
Bc	*D. bisectus*	U1333C-18H-5	105	U1333C-18H-5	85	146,290	146,090	172,790	172,590	172,790	172,590	172,690	0,100	C18r	C18r	40,432	40,410	40,421	0,011
T	*S. furcatolithoides*	U1333C-18H-6	137	U1333C-18H-6	115	148,110	147,890	174,610	174,390	174,610	174,390	174,500	0,110	C18r	C18r	40,626	40,602	40,614	0,012
B	*R. umbilicus*	U1333C-20H-3	25	U1333C-20H-2	25	157,350	155,850	185,300	183,800	185,300	183,800	184,550	0,750	C19r	C19r	42,012	41,647	41,829	0,182

Depth scales:
mbsf = meters below seafloor as measured by the drill pipe on Expedition 320
rmcd = revised meters composite depth (also referred to as revised CCSF-A). This is based on correlation between holes U1333A, B, and C from Westerhold et al. (2012
armcd = adjusted revised meters composite depth (also referred to as adjusted revised CCSF-A). Adjustments made to the rmcd to improve between hole correlation from Westerhold et al. (2012)
[1] Ages are based on magnetostratigraphy of Site U1333 from Acton et al. (unpublished data) and the composite GPTS of Expedition 320 (lilike et al. 2010).
The composite timescale is based on GPTS2004 (Lourens et al., 2004) from C6n down to the base of C6n.2n, on Pälike et al. (2006) down to the base of C19n, and on Cande and Kent (1995) for older chron
* Chron Base gives the chron in which the sample base occurs. Chron Top gives the chron in which the sample top occurs

The Top of *Chiasmolithus grandis*

The Top of *C. grandis* defines the base of CP15a Zone (Okada and Bukry 1980). The species is previously reported to be common at low to middle latitudes (Wei and Wise 1990a) but shows low frequencies and discontinuous presence, albeit counted in 9mm^2, at Hole 1333C. At this hole, *C. grandis* is present from the base of the section up to the upper part of Chron C18n.1n (158.55 ± 0.20 armcd; Table 1). Recent data from middle latitudes suggests a significant decrease in abundance of this taxon, that the authors named Highest Common Occurrence (HCO), just in the upper part of Chron C18n.1n (Fornaciari et al. 2010). Our results on the Top of *C. grandis* seem to be consistent with this, but provide an older age estimate for the last occurrence of this species, observed at Chron C17n.2n by the same authors (text-fig. 04). At Hole 1333C, the extinction of *C. grandis* thus occurs well before most of the published calibrations, except for findings of Monechi and Thierstein (1985), which observed the final presence of this taxon in the upper part of Chron C18n in the Mediterranean area. On this basis, we find that this biohorizon is either diachronous or inconsistent and should thus be used with caution.

The Base and Base common of *Isthmolithus recurvus*

The Base of *I. recurvus* defines the base of NP19-NP20 Zone and CP15b Subzone (Martini 1971; Okada and Bukry 1980). Data available from the literature provide a peculiar abundance pattern for this species, a first occurrence (B) lying within Chron C17n.1n is followed by a temporary absence and eventually by a common and continuous presence (Bc) of this taxon (Backman 1987; Catanzariti et al. 1997; Villa et al. 2008; Fornaciari et al. 2010; Fioroni et al. 2012). At Hole 1333C, *I. recurvus* is extremely rare and the first specimens ascribable to this taxon were recorded only in basal part of Chron C16n.2n (143.75 ± 0.50 armcd; Table 1), where the Bc of this species was usually found to occur (e.g., Fornaciari et al. 2010). The absence of this taxon before Chron C16n.2n is likely explained by its unevenly distribution in equatorial Pacific due to its preferences for cooler waters (e.g., Berggren et al. 1995).

The Top of *Discoaster saipanensis*

The Top of *Discoaster saipanensis* marks the base of Zone NP21 (Martini 1971), whereas the Tops of *D. saipanensis* and *D. barbadiensis,* define the base of Subzone CP16a (Okada and Bukry 1980). At Hole 1333C, the Top of the latter two species are well recorded at 136.92 armcd (136.35 ± 0.50 armcd; Table I) within Chron C13r. The extinction of rosette-shaped discoasters is clearly diachronous if high and low-middle latitude data are compared (Wei and Wise 1990a; Arney and Wise 2003; Persico and Villa 2004; Villa et al. 2008). In fact, this event has an age of ca. 40 Ma at ODP Site 748 (Villa et al. 2008, Fioroni et al. 2012) but is found consistently within Chron C13r at low-middle latitudes (Berggren et al. 1995). Our data from Hole 1333C support the idea that the disappearance of rosette-shaped discoasters at high latitudes was environmentally controlled and considerably precedes the final presence of these taxa at low-middle latitudes.

The Acme of *Clausicoccus subdistichus*

The Top of increased abundance (Ti) of *Clausicoccus subdistichus* defines the base of the CP16b Subzone (Okada and Bukry 1980). *Clausicoccus subdistichus* is reported to be quite common in the basal Oligocene of some sections while it can be very rare or absent in others (Perch-Nielsen 1985). Following Backman (1987), we instead use the Base of increased abundance (Bi) of *Clausicoccus subdistichus* both to subdivide the NP21 Zone and mark the base of the CP16b Subzone. This biohorizon seems to represent the best available nannofossil marker to approximate the base of the Oligocene being consistently found in the upper part of Chron C13r (e.g., Backman 1987; Coccioni et al. 1988; Berggren et al. 1995, Marino and Flores 2002; Hyland et al. 2009). At Hole 1333C, *C. subdistichus* and *Clausicoccus* generally show a notable increase in abundance at 134.45 armcd (135.35 ± 0.50 armcd; Table 1) and remain abundant up to the top of the studied section. The Bi of *C. subdistichus* is thus a clear event that can serve to approximate the Eocene-Oligocene boundary. However, the Ti of *C. subdistichus* is not well defined, because specimens ascribable to this taxon are still present and common even after the Top of *Ericsonia formosa* (128.17 ± 1.53 armcd), well above the base of the Oligocene.

The Top of *Ericsonia formosa*

The Top of *E. formosa* defines the base of NP22 Zone and CP16c Subzone (Martini 1971; Okada and Bukry 1980). This event is considered diachronous between low-mid latitudes (Nocchi et al. 1986; Premoli et al. 1988; Backman 1987; Berggren et al. 1995; Marino et al. 2002b), where it was found to occur from the uppermost part of Chron C13n and lower part of Chron C12r, and southern high latitudes, where it is present up to Chron C18 (Berggren et al. 1995).

APPENDIX 1
Taxonomic list.

Blackites gladius (Locker 1967) Varol, 1989
Chiasmolithus altus Bukry and Percival, 1971
Chiasmolith consuetus (Bramlette and Sullivan) Hay and Mohler, 1967
Chiasmolithus oamaruensis (Deflandre, 1954) Hay et a., 1966
Chiasmolithus grandis (Bramlette and Riedel) Radomski, 1968
Chiasmolithus solitus (Bramlette and Sullivan) Locker, 1968
Clausicoccus subdistichus (Roth and Hay, in Hay et al., 1967) Prins, 1979
Coccolithus cachaoi (Bown, 2005)
Coccolithus eopelagicus (Bramlette and Riedel) Bramlette and Sullivan, 1961
Coccolithus pelagicus (Wallich) Schiller, 1930
Cribrocentrum erbae (Fornaciari et al., in Fornaciari et al., 2010)
Cribrocentrum isabellae (Catanzariti et al., in Fornaciari et al., 2010)
Cyclicargolithus (Bukry, 1971)
Dictyococcites (Black, 1967)
Dictyococcites bisectus (Hay, Mohler and Wade) Bukry and Percival, 1971
Dictyococcites hesslandi (Haq) Haq and Lohmann, 1976
Discoaster barbadiensis Tan, 1927
Discoaster bifax Bukry, 1971
Discoaster binodosus Martini, 1958
Discoaster deflandrei Bramlette and Riedel, 1954
Discoaster gemmifer Stradner, 1961
Discoaster lenticularis Bramlette and Sullivan, 1961
Discoaster lodoensis Bramlette and Riedel, 1954
Discoaster mirus Deflandre, 1969
Discoaster saipanensis Bramlette and Riedel, 1954
Discoaster strictus Stradner, 1961
Discoaster subodoensis Bramlette and Sullivan, 1961
Discoaster tanii Bramlette & Riedel, 1954
Discoaster tanii var. *nodifer* (Bramlette and Riedel 1954)
Discoaster wemmelensis Achuthan and Stradner, 1969
Ericsonia formosa (Kamptner 1963) Hai 1971
Ericsonia subpertusa Hay and Mohler, 1967
Helicosphaera bramlettei (Müller) Jafar and Martini, 1975
Helicosphaera compacta Bramlette and Wilcoxon, 1967
Helicosphaera dinesenii Perch-Nielsen, 1971
Helicosphaera heezenii (Bukry) Jafar and Martini, 1975
Hughesius (Varol, 1989)
Isthmolithus recurvus Deflandre, 1954
Lanternithus minutus Stradner, 1962
Neococcolithes minutus (Perch-Nielsen) Perch-Nielsen, 1971
Pontosphaera multipora (Kamptner) Roth, 1970
Pseudotriquetrorhabdulus Wise in Wise and Constans, 1976
Reticulofenestra Hay et al., 1966
Reticulofenestra daviesii (Haq) Haq, 1971
Reticulofenestra umbilicus (Levin), Martini and Ritzkowski, 1968
Rhabdolitus Kamptner ex Deflandre in Grass, 1952
Sphenolithus distentus (Martini) Bramlette and Wilcoxon, 1967
Sphenolithus furcatolithoides Locker, 1967
Sphenolithus intercalaris Martini, 1976
Sphenolithus moriformis (Brönnimann and Stradner) Bramlette and Wilcoxon, 1967
Sphenolithus obtusus Bukry, 1971
Sphenolithus radians Deflandre, 1952
Sphenolithus richteri Bown and Dunkley Jones, 2012
Sphenolithus spiniger Bukry, 1971
Thoracosphaera Kamptner, 1927
Toweius eminens Bramlette and Sullivan, 1961
Transversopontis Hay, Mohler and Wade, 1966
Watznaueria Reinhardt 1964

At Hole 1333C, the species was quite common and its final presence was observed at the Chron13n/C12r transition (128.75 ± 2.11 armcd; Table 1), consistent with most of the low-mid latitude data available and additional data from the equatorial Pacific (Bown and Dunkley Jones 2012).

Additional calcareous nannofossil biohorizons

In the equatorial Pacific, poor preservation of study material and low abundances for a number of marker species utilized in standard zonations prevent a full recognition of all standard biohorizons, which thus implies a poor biostratigraphic resolution. To improve this, we have integrated standard bioevents with some additional calcareous nannofossil datums recently proposed by Catanzariti et al. (1997) and Fornaciari et al. (2010). Comments on these additional biohorizons are provided in the following in stratigraphic order:

The Base, Base common and Top of *Cribrocentrum reticulatum*

The appearance and disappearance datums of this species have been employed in middle-late Eocene regional biostratigraphy (Wei and Wise 1989, 1990a, Berggren et al. 1995; Catanzariti et al. 1997, Marino and Flores 2002, Fornaciari et al. 2010) and its first appearance has been proposed for approximating the base of the Bartonian (Berggren et al. 1995; Flugeman 2007). Published calibrations for the first appearance of *C. reticulatum* are not consistent, ranging from Chron C20r to Chron C18n, likely because of rare and discontinuous presence of *C. reticulatum* in its initial stratigraphic distribution (see discussion in Fornaciari et al. 2010). However, the B_c of *C reticulatum* has been consistently found at the base of Chron C18r and seem to be a more reliable biohorizon (Berggren et al. 1995; Fornaciari et al. 2010). Unfortunately at Hole 1333C strong dissolution in calcareous nannofossil specimens often produces the partial/total loss of the central area, which inhibits straightforward recognition and reliable distribution patterns for this taxon (see also Bown and Dunkley Jones 2012). The same reasoning holds true even for the Top of this taxon at least in equatorial Pacific material preventing determination of this biohorizon.

The Top of *Sphenolithus furcatolithoides*

The Top of *S. furcatolithoides* is one of the clearest biohorizons of the late part of the middle Eocene and it is consistently found in the upper part of Chron C18r shortly preceding the Bc of *D. bisectus* and *D. hesslandii* (Proto Decima et al. 1975; Perch-Nielsen 1977; Parisi et al. 1988; Nocchi et al. 1988; Firth 1989; Wei and Wise 1989; 1992; Okada 1990; Bralower and Mutterlose 1995; Mita 2001; Marino and Flores 2002a; b). At IODP Hole 1333C, *S. furcatolithoides* goes extinct in the upper part of Chron C18r (174.50 ± 0.11 armcd; Table 1) just before the Bc of *D. bisectus* and *D. scrippsae* thus maintaining the same stratigraphic position even in this area.

The Base common of *Dictyococcites bisectus*

The taxonomic ambiguities in defining *D. bisectus* essentially derive from different morphometric definitions. Here, we have decided to follow the generally accepted advice of Bralower and Mutterlose (1995), who proposed 10μm as lower limit for the size of this taxon. This clarification makes the biostratigraphic use of *D. bisectus* more useful. Although some specimens of *D. bisectus* have been reported before Chron C18r (Mita 2001; Larrasoaña et al. 2008), the remarkable increase in abundance in the upper part of Chron C18r is considered to be a very promising datum since it is associated with two other clear biohorizons (i.e., the Bc of *D. hesslandii* and the Top of *S. furcatolithoides*). At Hole 1333C, the Bc of *D. bisectus* has been observed in the upper part of Chron C18r (172.69 ± 0.10 armcd; Table 1), consistent with previous results (e.g., Backman 1987; Bralower and Mutterlose 1995; Fornaciari et al. 2010), and very close to the onset of the MECO event. This large dataset indicates that this biohorizon is one of the more reliable bioevents of this interval.

The Base common of *Dictyococcites hesslandii*

The Bc of *D. hesslandii* is one of the biohorizons found close to the Bc of *D. bisectus* in the upper part of Chron C18r, during the MECO event (Backman 1987; Fornaciari et al. 2010). Since this species has a problematic taxonomy, we clarify our taxonomic concept of *D. hesslandii,* which includes specimens smaller than 10 µm, with an elliptical outline, a solid central area composed by radial calcite elements and continuous extinction lines (see also Fornaciari et al. 2010). At Hole 1333C this taxon shows is common and consistently present from the upper part of Chron C18r (172.69 ± 0.11 armcd; Table 1) and coincident with the prominent increase in abundance of *D. bisectus*. This datum represents a good biohorizon especially if used together with the Bc of *D. bisectus* and the Top of *S. furcatolithoides*.

The Top common of *Sphenolithus spiniger*

The Tc of *S. spiniger* has been recently considered by Fornaciari et al (2010) in their new biozonation. This taxon shows a rare

and discontinuous presence in the poorly preserved material recovered at Hole 1333C. However, data available from Hole 1333A (Bown and Dunkley Jones 2012) show that *S. spiniger* disappears close to the Top of *S. furcatolithoides* coincident with a barren to semi-barren interval correlative to the MECO. This pattern is consistent with data reported in low-mid latitude areas (e.g. Fornaciari et al. 2010).

The Base and Top of *Sphenolithus obtusus*

The stratigraphic distribution of *S. obtusus* has been constrained in the middle Eocene by a number of previous works (Bukry 1973; Nocchi et al. 1988; Wei and Wise 1989; 1992; Okada 1990). In particular, Fornaciari et al. (2010) use the Base and Top of this taxon to redefine and subdivide the NP17 Zone of Martini (1971). These authors report the Base of *S. obtusus* in the lower part of Chron C18n at the transition between Chron C18n.1n and Chron C17r. Our data from Hole 1333C confirm the same positions with respect to the GPTS, which are the lower part of Chron C18n.1n for the Base (164.15 ± 0.20 armcd; Table 1) and uppermost part of Chron C18n.1n for the Top (158.15 ± 0.20 armcd; Table 1), respectively.

The Acme of *Cribrocentrum erbae* and the Base of *Cribrocentrum isabellae*

The Bi of *Cribrocentrum erbae* and the Base of *Cribrocentrum isabellae* have been proposed by Fornaciari et al. (2010) to redefine and subdivide the NP18 Zone of Martini (1971). These biohorizons seem to be extremely reliable at least at low-mid latitudes, however, the strong dissolution in the deep equatorial Pacific have biased the assemblage, virtually removing all the specimens belonging to genus *Cribrocentrum*. Nevertheless, data available from the shallower Site U1334 have confirm the presence of an acme of *C. erbae* at the base of Zone NP18 (Bown and Dunkley Jones 2012), suggesting that this biohorizon is still to be considered very promising.

The Acme of *Sphenolithus intercalaris*

Martini (1971) formally describes *S. intercalaris* from sediments recovered during DSDP Leg 33 in the Central Pacific giving a biostratigraphic distribution restricted between NP16 Zone and NP21 Zone (middle-late Eocene to early Oligocene; 1976). Perch-Nielsen (1985) reported an even more limited distribution in Zones NP17-NP18. However, more recently Bown (2005) found this taxon to be present in the upper Eocene-lower Oligocene sediments recovered at the Shatsky Rise (Northwest Pacific). Our data from Hole 1333C are consistent with previous results from the Pacific Ocean (Martini 1976; Bown 2005) and provide evidence for a remarkable increase of *S. intercalaris* between 143.75 and 136.35 armcd (NP21 Zone or MNP21A Zone; Table 1), where this taxon represents more than 50% of the total assemblage of the sphenoliths. This interval is here referred to as the Acme of *S. intercalaris* and correlates with the late part of the Priabonian just preceding the Eocene-Oligocene boundary. This biohorizon is prominent at Hole 1333C but should be tested over wider areas in order to be used for regional correlations.

CONCLUSIONS

A high-resolution calcareous nannofossil biostratigraphy was carried out at Hole 1333C in the equatorial Pacific Ocean. The middle Eocene-early Oligocene study section encompasses nannofossil Zones NP15–NP22 and Chrons C20r–C12r. We have analyzed more than 20 biohorizons in an 11 Myr time interval, from ca 44 Ma to 33 Ma. A number of these biohorizons are used in standard zonations (Martini 1971; Okada and Bukry 1980) but not all of them are usable in our material because of the uneven distribution of some marker species. For this reason we tested additional bioevents and some of these proved to be reliable and reproducible over wide areas, including the Top of *S. furcatolithoides*, the Base and Top of *S. obtusus* and the Bc of *D. hesslandii* and *D. bisectus*. However, others are affected by the pervasive dissolution of the study material, which has profoundly altered the abundance of taxa, especially those more prone to dissolution. The preservation of carbonate sediments is an important issue in the equatorial Pacific because it is highly variable during the Eocene, where several shallowing events of the CCD, mirroring the $CaCO_3$ content, are found to occur. Calcareous nannofossil absolute and relative abundance can be used as a proxy of degree of dissolution of the assemblage/ changes and thus of carbonate preservation through time.

ACKNOWLEDGMENTS

This research used samples and data provided by the Ocean Drilling Program (ODP). ODP is sponsored by the U.S.

PLATE 1

Microphotographs of calcareous nannofossil from the ODP Leg 320, Site U1333 in the middle and late Eocene interval. All specimens ×1000.

1-2 *Coccolithus eopelagicus*. Sample 320-U1333C-16H-3W, 45 1 Crossed nicols. 2 Parallel light, 3-4. *Coccolithus pelagicus*. Sample 320-U1333C-18H-8W, 15.

3 Crossed nicols.

4 Parallel light.

5-6 *Ericsonia formosa*. Sample 320-U1333C-14H-1W, 135. 5 Crossed nicols. 6 Parallel light.

7-8 *Coccolithus cachaoi* Sample 320-U1333C-20H-6W, 75. 7 Crossed nicols. 8 Parallel light.

9-10 *Chiasmolithus solitus*. Sample 320-U1333C-17H-3W, 35. 9 Crossed nicols. 10 Parallel light.

11-12 *Chiasmolithus grandis*. Sample 320-U1333C-17H-3W, 35. 11 Crossed nicols. 12 Parallel light.

13-14 *Chiasmolithus grandis*. Sample 320-U1333C-17H-2W, 45. 13 Crossed nicols. 14 Parallel light.

15-16 *Dictyococcites bisectus*. Sample 320-U1333C-18H-5W, 65. 15 Crossed nicols. 16 Parallel light.

17 *Dictyococcites hesslandii*. Sample 320-U1333C-15H-5W, 95. Crossed nicols.

18 *Cyclicargolithus floridanus*. Sample 320-U1333C-20H-2W, 25. Crossed nicols.

19 *Reticulofenestra umbilicus*. Sample 320-U1333C-18H-8W, 75. 19 Crossed nicols. 20 Parallel light.

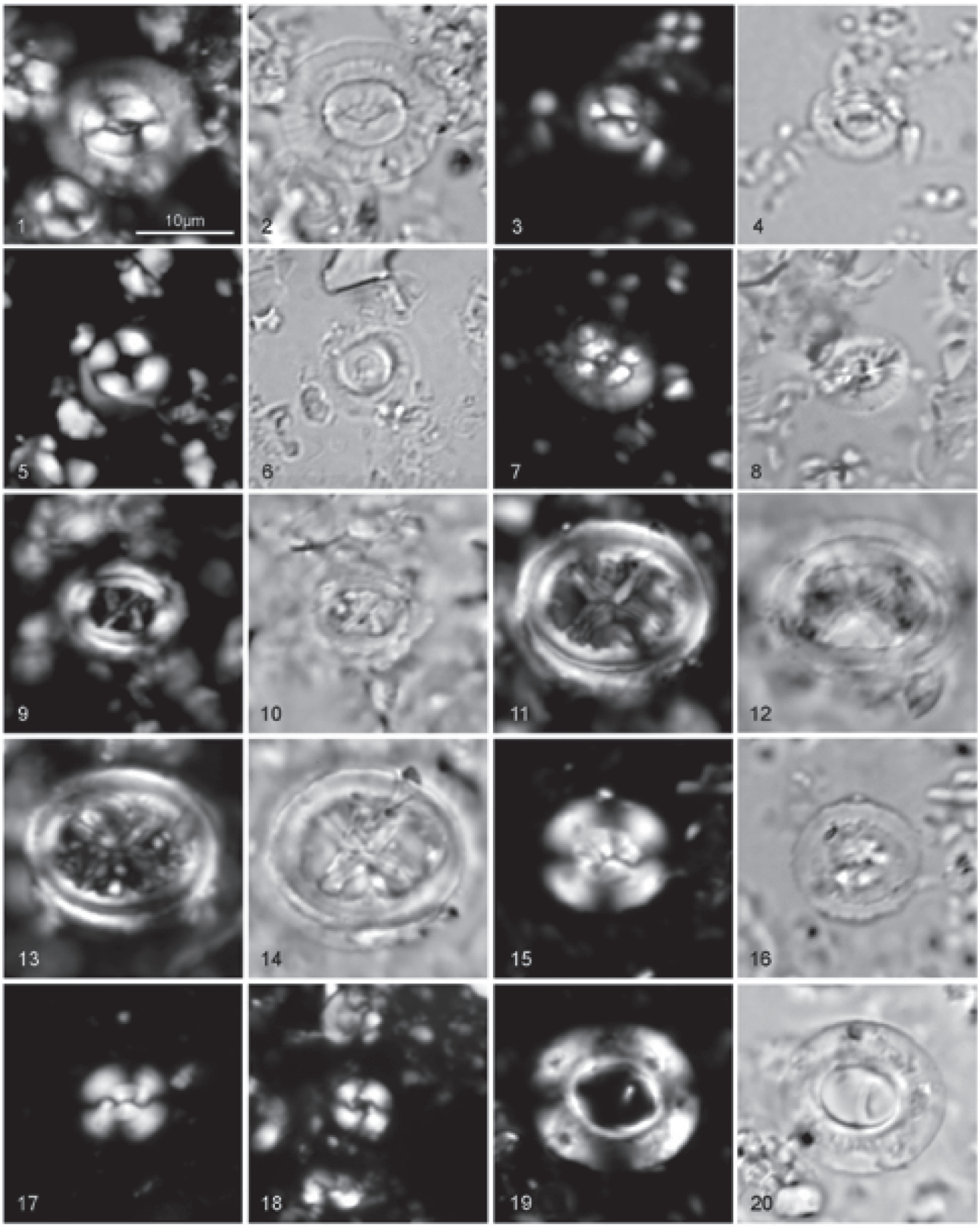
1
10µm
2
3
4
5
6
7
8
9
10
11
12
13
14
15
16
17
18
19
20

National Science Foundation (NSF) and participating countries under management of Joint Oceanographic Institution (JOI) Inc. We would like to thank two anonymous reviewers and the Micropaleontology associated Editor, Marci Robinson, for their careful reviews of the manuscript. FT, CA and DR were funded by MIUR-PRIN grant 2007W9B2WE_004. Additional funding was provided to CA and FT by UniPD – CPDA095875 (2009). Paleomagnetism results for Site U1333 (GA) were supported by the National Science Foundation under Grant Number (NSF OCE-0961412). TW was funded by the Deutsche Forschungsgemeinschaft (DFG).

REFERENCES

ADELSECK, C. G. JR., GEEHAN, G. W. and ROTH, P. H., 1973. Experimental evidence for the selective dissolution and overgrowth of calcareous nannofossils during diagenesis. *Geological Society of America Bulletin*, 84: 2755–2762.

AGNINI C., FORNACIARI E., GIUSBERTI L., GRANDESSO P., LANCI L., LUCIANI V., MUTTONI G., RIO D., STEFANI C., PÄLIKE H. and SPOFFORTH D. J. A, 2011. Integrated biomagnetostratigraphy of the Alano section (NE Italy): a proposal for defining the Middle–Late Eocene boundary. *Geological Society of America Bulletin*, 123: 841–872.

ARNEY, J. E . and WISE, S. W., Jr., 2003. Paleocene–Eocene nannofossil biostratigraphy of ODP Leg 183, Kerguelen Plateau. In: Frey, F. A., Coffin, M. F., Wallace, P. J . and Quilty, P. G., Eds., *Proceedings of the Ocean Drilling Project, Scientific Results, 183,* 1–59. College Station TX: Ocean Drilling Program.

AUBRY, M.-P., 1984. *Handbook of Cenozoic calcareous nannoplankton, Book 1, Ortholithae (Discoaster)*. New York: Micropaleontology Press, 263 pp.

———, 1988. *Handbook of Cenozoic calcareous nannoplankton, Book 2, Ortholithae (Holococcoliths, Ceratoliths, Ortholiths and Other)*. New York: Micropaleontology Press. 279 pp.

———, 1989. *Handbook of Cenozoic calcareous nannoplankton, Book 3, Ortholithae (Pentaliths and other), Heliolithae (Fasciculiths, Sphenoliths and others)*. New York: Micropaleontology Press. 279 pp.

———, 1990. *Handbook of Cenozoic calcareous nannoplankton, Book 4, Heliolithae (Helicoliths, Cribriliths, Lopadoliths and others)*. New York: Micropaleontology Press. 381 pp.

———, 1992. Late Paleogene calcareous nannoplankton evolution: a tale of climatic deterioration, in Eocene–Oligocene climatic and biotic evolution. In: Prothero, D. R. and Berggren, W. A., Eds., *Eocene–Oligocene climatic and biotic evolution*, 272–309. Princeton, NJ: Princeton University Press.

———, 1998, Early Paleogene calcareous nannoplankton evolution: a tale of climatic amelioration, in late Paleocene and early Eocene climatic and biotic evolution. In: Aubry, M.-P., Lucas, S. and Berggren, W. A., Eds., *Late Paleocene–early Eocene climatic and biotic events in the marine and terrestrial record*, 158–203. New York: Columbia University Press.

———, 1999. *Handbook of Cenozoic calcareous nannoplankton, Book 5, Heliolithae (Zygoliths and Rhabdoliths)*. New York: Micropaleontology Press, 368 pp.

AUBRY, M.-P. and BORD, D., 2009. Reshuffling the cards in the photic zone at the Eocene/Oligocene bundary. In: Koeberl, C., and Montanari, A., Eds., *The Late Eocene Earth: Hot House, Ice House, and Impacts,* 279–301. Boulder: Geological Society of America. Special Paper 452:

BACKMAN, J., 1986. Late Paleocene to middle Eocene calcareous nannofossil biochronology from the Shatsky Rise, Walvis Ridge and Italy. *Palaeogeography, Palaeoclimatology, Palaeoecology*. 57: 43–59.

———, 1987. Quantitative calcareous nannofossil biocronology of middle Eocene through early Oligocene sediments from DSDP Sites 522 and 523. *Abhandlungen der Geologischen Bundesanstalt*, 39: 21–31.

BACKMAN, J . and HERMELIN. J. O., 1986. Morphometry of the Eocene nannofossil Reticulofenestra umbilicus lineage and its biochronological consequences. *Palaeogeography, Palaeoclimatology, Palaeoecology*, 57: 103–116.

PLATE 2

Microphotographs of calcareous nannofossil from the ODP Leg 320, Site U1333 in the Middle and Late Eocene interval. All specimens ×1000.

1 *Clausicoccus subdistichus*; Sample 320-U1333C-14H-4W, 5. Crossed nicols.

2-4 *Sphenolithus furcatolithoides*. Sample 320-U1333C-18H-6W, 137. 2. Crossed nicols 0°. 3. Crossed nicols 30°. 4. Crossed nicols 45°.

5 *Sphenolithus moriformis*. Sample 320-U1333C-18H-8W, 35. Crossed nicols 0°.

6-8 *Sphenolithus cf. richteri*. Sample 320-U1333C-18H-7W, 145. 6. Crossed nicols 0°. 7. Crossed nicols 30°. 8. Crossed nicols 45°.

9-11 *Sphenolithus predistentus* / *S. distentus* intergrade. Sample 320-U1333C-13H-7W, 70. 9. Crossed nicols 0°. 10. Crossed nicols 30°. 11. Crossed nicols 45°.

12 *Thoracosphaera sp.*; Sample 320-U1333C-17H-4W, 125. Crossed nicols.

13-15 *Sphenolithus obtusus*. Sample 320-U1333C-17H-5W, 115. 13. Crossed nicols 0°. 14. Crossed nicols 30°. 15. Crossed nicols 45°.

16 *Discoaster saipanensis*; Sample 320-U1333C-4H-1W, 135. Crossed nicols.

17 *Discoaster barbadiensis*; Sample 320-U1333C-4H-1W, 135. Crossed nicols.

18 *Discoaster deflandrei*; Sample 320-U1333c-14H-3W, 55. Crossed nicols.

19-20 *Isthmolithus recurvus*. Sample 320-U1333C-14H-7W, 65. 19 Crossed nicols. 20 Parallel light.

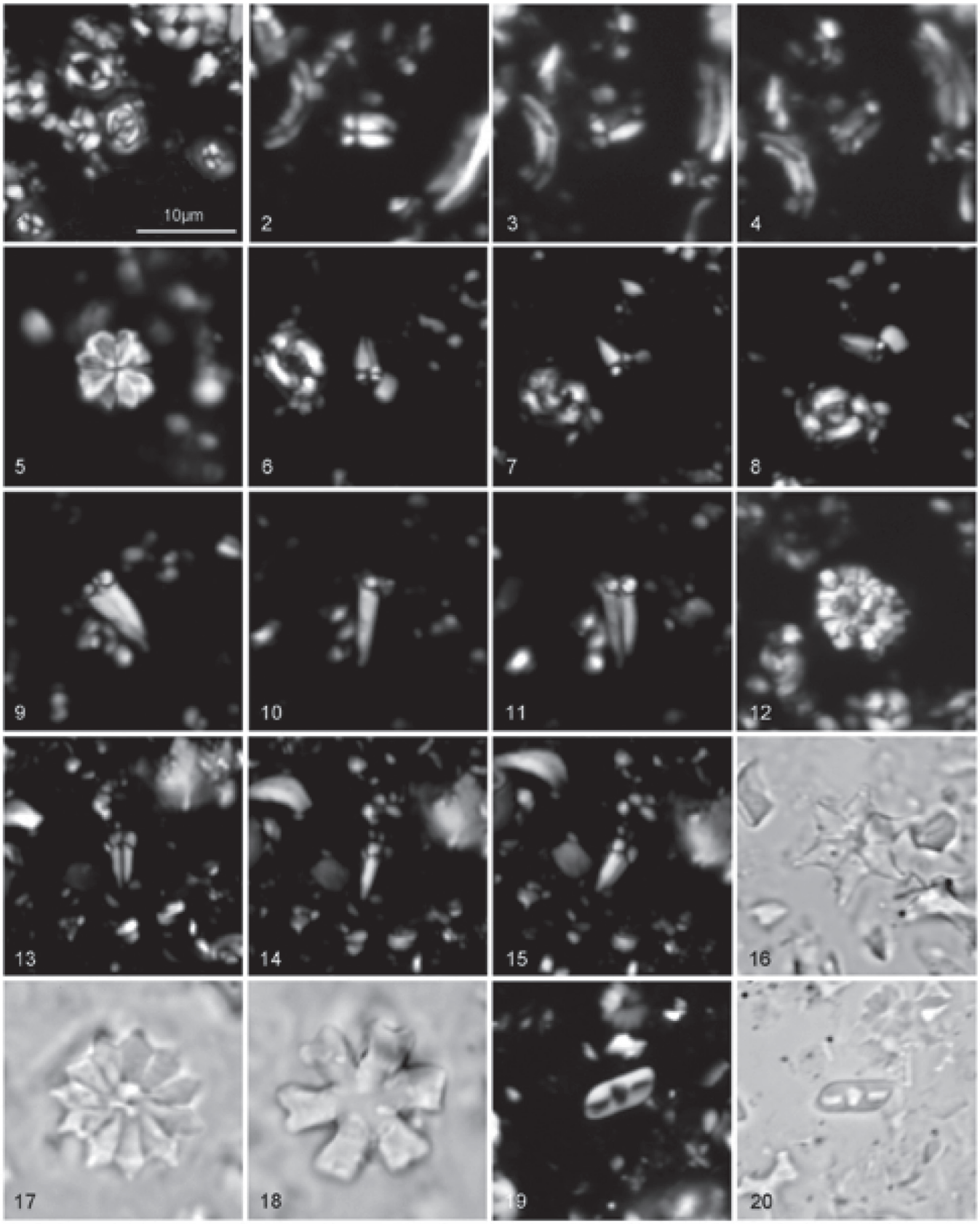
10µm
2
3
4
5
6
7
8
9
10
11
12
13
14
15
16
17
18
19
20

BACKMAN, J., RAFFI, I., RIO, D., FORNACIARI, E., PÄLIKE, H., 2012. Biozonation and biochronology of Miocene through Pleistocene calcareous nannofossils from low and mid latitude. *Newsletters on Stratigraphy*, 45: 221–244.

BERGGREN, W. A., KENT, D. V., SWISHER, C. C. and AUBRY M. P., 1995. A revised Cenozoic geochronology and chronostratigraphy. In: Berggren, W. A., Kent, D. V., Hardenbol, J., Eds., *Geochronology, time scales and global stratigraphic correlation,* 129-212. Tulsa: Society for Economic Paleontology and Mineralogy. Special Publication 54.

BOHATY, S. M. and ZACHOS, J. C., 2003. Significant Southern Ocean warming event in the late middle Eocene. *Geology*, 31: 1017– 1020

BOHATY, S. M., ZACHOS, J. C., FLORINDO, F. and DELANEY, M. L., 2009. Coupled greenhouse warming and deep–sea acidification in the middle Eocene *Paleoceanography*, 24: PA2207.

BORNEMANN, A. and MUTTERLOSE, J., 2008. Calcareous nannofossil and $\delta^{13}C$ records from the early Cretaceous of the Western Atlantic Ocean: Evidence for enhanced fertilization across the Berriasian–Valanginian transition. *Palaios*, 23: 821–832.

BOWN, P. R., 2005. Cenozoic calcareous nannofossil biostratigraphy, ODP Leg 198 Site 1208 (Shatsky Rise, northwest Pacific Ocean). In Bralower, T. J., Premoli Silva, I . and Malone, M. J., Eds., *Proceedings of the Ocean Drilling Program, Scientific Results, 198*, 1-44. College Station, TX: Ocean Drilling Program.

BOWN, P. R. and DUNKLEY JONES, T., 2012. Calcareous nannofossils from the Paleogene equatorial Pacific (IODP Expedition 320 Sites U1331–1334). *Journal of Nannoplankton Research*, 32: 3–51.

BOWN, P. R. and YOUNG, J. R., 1998. Techniques. In: Bown, P. R., Ed., *Calcareous nannofossil biostratigraphy,* 16-28. London: Chapman & Hall.

BOWN, P. R., LEES, J. A . and YOUNG, J. R., 2004. Calcareous nannoplankton evolution and diversity through time.. In: Thierstein, H. R. and Young, J. R., Eds., *Coccolithophores - from molecular processes to global impact,* 481–505. London: Springer-Verlag.

BRALOWER, T. J. and MUTTERLOSE, J., 1995. Calcareous nannofossil biostratigraphy of ODP Site 865, Allison Guyot, Central Pacific Ocean: a tropical Paleogene reference section. In Winterer, E. L., Sager, W. W., Firth, J. V., et al., *Proceedings of the Ocean Drilling Program, Scientific Resuls*, *143,* 31–72. College Station, TX: Ocean Drilling Program.

BUKRY, D., 1971. Cenozoic calcareous nannofossils from the Pacific Ocean. *Transactions of the San Diego Society of Natural History*, 16: 303–328.

———, 1973. Coccolith stratigraphy, eastern equatorial Pacific, Leg 16, Deep Sea Drilling Project. In: van Andel, T. H., Heath, G. R. et al., et al., *Deep Sea Drilling Project Initial Reports, 16:* 653–711. Washington DC: US Government Printing Office.

CANDE, S. C. and KENT, D. V., 1995. Revised calibration of the geomagnetic polarity time scale for the Late Cretaceous and Cenozoic. *Journal of Geophysical Research,* 100 (B4): 6093–6096.

CATANZARITI, R., RIO, D. and MARTELLI, L., 1997. Late Eocene to Oligocene calcareous nannofossil biostratigraphy in northern Apennines: the Ranzano Sandstones. *Memorie di Scienze Geologische,* 49: 207–253.

COCCIONI, R., 1988. The genera *Hantkenina* and *Cribrobantkenina* (Foraminifera) in the Massignano section (Ancona, Italy). In: Premoli Silva I., Coccioni R. and Montanari A., Eds., The Eocene-Oligocene Boundary in the March-Umbria Basin (Italy), 81–96. Ancona: Fratelli Anniballi. International Union of Geological Sciences, International Subcommission on Paleogene Stratigraphy, Special Publication.

COXALL, H. K., WILSON, P. A., PÄLIKE, H., LEAR, C. H. and BACKMAN, J., 2005. Rapid stepwise onset of Antarctic glaciations and deeper calcite compensation in the Pacific Ocean. *Nature* , 433: 53–57.

DECONTO, R. M., POLLARD, D., WILSON, P. A., PÄLIKE, H., LEAR, C. H. and PAGANI, M., 2008. Thresholds for Cenozoic bipolar glaciation. *Nature,* 455: 652–656.

EDGAR, K. M., WILSON, P. A., SEXTON, P. F. and SUGANUMA, Y., 2007. No extreme bipolar glaciation during the main Eocene calcite compensation shift. *Nature*, 448: 908–911.

FIORONI, C. VILLA, G., PERSICO, D., WISE, S. W. and PEA, L., 2012. Revised middle Eocene–upper Oligocene calcareous nannofossil biozonation for the Southern Ocean. *Revue de micropaléontologie*, 55: 53–70.

FIRTH, J. V., 1989. Eocene and Oligocene calcareous nannofossils from the Labrador Sea, ODP Leg 105. In: Srivastava, S. P., Arthur, M., Clement, B. et al., *Proceedings of the Ocean Drilling Program, Scirntific Results, 105, 263-286*. College Station, TX: Ocean Drilling Program.

FLUEGEMAN, R. H., 2007. Unresolved issues in Cenozoic chronostratigraphy. *Stratigraphy*, 4: 109–116.

FORNACIARI, E., AGNINI, C., CATANZARITI, R., RIO, D., BOLLA, E. M. and VALVASONI, E., 2010. Mid–latitude calcareous nannofossil biostratigraphy, biochronology and evolution across the middle to late Eocene transition. *Stratigraphy* 7: 229–264.

GRADSTEIN, F. M., OGG, J. G., SCHMITZ, M. D. and OGG, G. M., Eds., 2012. *The Geological Time Scale 2012*. Amsterdam: Elsevier, 1144p.

HASSENKAM, T., JOHNSSON, A., BECHGAARD, K. and STIPP S. L. S., 2011. Tracking single coccolith dissolution with picogram resolution and implications for CO_2 sequestration and ocean acidification. *Proceedings of the National Academy of Sciences,* 108: 8571–8576.

HAY, W. W., 1970. Sedimentation rates: Calcium carbonate compensation. In: Bader, R. G., Gerard, R. D. et al., *Deep Sea Drilling Project Initial Reports*, *4*, 668–672. Washington, DC: Government Printing Office.

HENRIKSEN, K., YOUNG, J. R., BOWN, P. R. and STIPP, S. L. S., 2004. Coccolith biomineralisation studied with atomic force microscopy. *Palaeontology*, 47: 725–743.

HYLAND, E., MURPHY, B., VARELA, P., et al., 2009. Integrated stratigraphic and astrochronologic calibration of the Eocene–Oligocene transition in the Monte Cagnero section (northeastern Apennines, Italy): A potential parastratotype for the Massignano global stratotype section and point (GSSP). In: Koeberl, C., and Montanari, A., Eds., *The Late Eocene Earth: Hot House, Ice House, and Impacts,* 303–322. Boulder: Geological Society of America. Special Papers, 452:

JOVANE L., FLORINDO, F., COCCIONI, R., DINARES-TURELL, J., MARSILI, A., MONECHI, S., ROBERTS, A. P. and SPROVIERI, M., 2007. The middle Eocene climatic optimum event in the Contessa Highway section, Umbrian Apennines, Italy. *Geological Society of America Bulletin*, 119: 413–427.

LARRASOAÑA, J. C., GONZALVO, C., MOLINA, E., MONECHI, S., ORTIZ, S., TORI, F. and TOSQUELLA, J., 2008. Integrated magnetobiochronology of the Early/Middle Eocene transition at Agost (Spain): Implications for defining the Ypresian/Lutetian boundary stratotype. *Lethaia*, 41: 395–415.

LYLE, M . and WILSON, P. A., 2006. Leg 199 synthesis: Evolution of the equatorial Pacific in the early Cenozoic. In: Lyle, M., and Firth, J., et al., *Proceedings of the Ocean Drilling Program, Scientific Results,* volume 199, pages 1-39. College Station, TX, Ocean Drilling Program.

LYLE, M., OLIVAREZ LYLE, A., BACKMAN, J. and TRIPATI, A., 2005. Biogenic sedimentation in the Eocene equatorial Pacific — the stuttering greenhouse and Eocene carbonate compensation depth. In: Lyle, M., and Firth, Eds., *Proceedings of the Ocean Drilling Program, Scientific results,* volume 199, pages 1-35. College Station, TX: Ocean Drilling Program.

LYLE, M., PÄLIKE, H., NISHI, H, RAFFI, I., GAMAGE, K., KLAUS, A. and THE IODP EXPEDITION320/321 SCIENTIFIC PARTY, 2010. The Pacific Equatorial Age Transect, IODP Expeditions 320 and 321: Building a 50-million-year-long environmental record of the Equatorial Pacific. *Scientific Drilling,* 9: 4–15.

LOURENS, L. J., HILGEN, F. J., SHACKLETON, N. J., LASKAR, J. and WILSON, D., 2004. The Neogene Period. In: Gradstein, F. M., Ogg, J. G. and Smith, A. G., Eds., *A Geological Time Scale 2004,* 409–440. Cambridge: Cambridge University Press.

MARINO, M. and FLORES, J. A., 2002a. Miocene to Pliocene calcareous nannofossil biostratigraphy at ODP Leg 177 Sites 1088 and 1090. *Marine Micropaleontology*, 45: 291–307.

———, 2002b. Middle Eocene to early Oligocene calcareous nannofossil stratigraphy at Leg 177 Site 1090. *Marine Micropaleontology,* 45: 383–398.

MARTINI, E., 1971. Standard Tertiary and Quaternary calcareous nannoplankton zonation. In: Farinacci, A., Ed., *Proceedings of the International Conference on Planktonic Microfossils*, *Volume 2*. 739–785. Roma: Edizione Tecnoscienza.

———, 1976. Cretaceous to Recent calcareous nannoplankton from the central Pacific Ocean (DSDP Leg 33). In Schlanger, S. O. and Jackson, E. D., et al., *Inituial Reports of the Deep Sea Drilling Project*, *33,* 439–450. Washington DC: Government Printing Office.

MILLER, K. G., WRIGHT, J. D. and FAIRBANKS, R. G., 1991. Unlocking the Ice House: Oligocene–Miocene oxygen isotopes, eustasy, and margin erosion. *Journal of Geophysical Research,* 96: 6829–6848.

MITA, I., 2001. Data Report: Early to late Eocene calcareous nannofossil assemblages of Sites 1051 and 1052, Blake Nose, northwestern Atlantic Ocean. In: Kroon, D., Norris, R. D. and Klaus, A., Eds., *Proceedings of the Ocean Drilling Program, Scientific Results, 171B*, 1–28. College Station, TX: Ocean Drilling Prgram.

MONECHI, S. and THIERSTEIN, H. R., 1985. Late Cretaceous–Eocene nannofossil and magnetostratigraphic correlations near Gubbio, Italy. *Marine Micropaleontology*, 9: 419–440.

NOCCHI, M., PARISI, G., MONACO, P., MONECHI, S. and MADILE, M., 1988. Eocene and Early Oligocene micropaleontology and paleoenvironments in SE Umbria, Italy. *Palaeogeography, Palaeoclimatology, Palaeoecology,* 67: 181–124.

NOCCHI, M., PARISI, G., MONACO, P., MONECHI, S., MADILE, M., NAPOLEONE, G., RIPEPE, M., ORLANDO, M., PREMOLI SILVA, I. and BICE, D. M., 1986. The Eocene–Oligocene boundary in the Umbrian pelagic sequences, Italy. In: Pomerol, Ch. and Premoli Silva, I., Eds., *Terminal Eocene events,* 25–40. Amsterdam: Elsevier. Developments in Palaeontology and Stratigraphy, 9

OKADA, H., 1990. Quaternary and Paleogene calcareous nannofossils, Leg 115. In: Duncan, R. A., Backman, J., Peterson, L. C., et al., *Proceedings of the Ocean Drilling Program, Scientific Results*, 115: 129–174. College Station, TX: Ocean Drilling Program.

OKADA, H . and BUKRY, D., 1980. Supplementary modification and introduction of code numbers to the low–latitude Coccolith biostratigraphic zonation, (Bukry, 1973; 1975). *Marine Micropaleontol*ogy, 5: 321–325

PÄLIKE, H., NORRIS R. D., HERRLE, J. O., WILSON, P. A., COXALL, H. K., LEAR, C. H., SHACKLETON, N. J., TRIPATI, A. K. and WADE, B. S., 2006. The heartbeat of the Oligocene cimate system. *Science*, 314: 1894–1898.

PÄLIKE, H., NISHI, H., LYLE, M., RAFFI, I., GAMAGE, K., KLAUS, A . and THE EXPEDITION 320/321 SCIENTISTS, 2010. Expedition 320/321 summary. In: Pälike, H., Lyle, M., Nishi, H., Raffi, et al., *Pacific equatorial transect,* 1-141. Tokyo: Integrated Ocean Drilling Program Management International, Inc. IODP Proceedings, 320/321.

PÄLIKE, H., NISHI, H., LYLE, M., RAFFI, I., KLAUS, A., GAMAGE, K . and THE EXPEDITION 320/321 SCIENTISTS, 2009. *Pacific equatorial transect*. Tokyo: Integrated Ocean Drilling Program Management International, Inc. IODP Prelimnary Reports, 320/321.

PÄLIKE, H., LYLE, M. W., NISHI, H., et al., 2012. A Cenozoic record of the equatorial Pacific carbonate compensation depth, *Nature*, 488: 609–615.

PERCH-NIELSEN, K., 1985 Cenozoic calcareous nannofossils. In: Bolli H. M., Saunders J. B. and Perch-Nielsen K., Eds., *Plankton stratigraphy,* 427–554. Cambridge: Cambridge University Press.

PARISI, G., GUERRERA, F., MADILE, M., MAGNONI, G., MONACO, P., MONECHI, S. and NOCCHI, M., 1988. Middle Eocene to early Oligocene calcareous nannofossil and foraminiferal Biostratigraphy in the Monte Cagnero section, Piobbico (Italy). In: Premoli Silva. I., Coccioni. R. and Montanari, A., Eds., *The Eocene–Oligocene boundary in the Marche–Umbria Basin (Italy),* 119–235. Ancona: Fratelli Anniballi. International Union of Geological Sciences, International Subcommission on Paleogene Stratigraphy, Special Publication.

PERCIVAL, S. F., 1984. Late Cretaceous to Pleistocene calcareous nannofossils from the South Atlantic oxygen and carbon isotope record from South Atlantic Deep Sea Drilling Project 73. In Hsu, K. J., La Brecque, J. L., et al., *Deep Sea Drilling Project, Initial Reports 73,* 391–424. Washington, DC: U. S. Government Printing Office.

PERSICO, D. and VILLA G., 2004. Eocene–Oligocene calcareous nannofossils from Maud Rise and Kerguelen Plateau (Antarctica): palaeoecological and palaeoceanographic implications. *Marine Micropaleontology*, 52: 153–179.

POORE, R. Z. and MATTHEWS, R. K., 1984. Late Eocene–Oligocene oxygen and carbon isotope record from South Atlantic Ocean DSDP Site 522. In: Hsu, K. J., La Brecque, J. L., et al., *Deep Sea Drilling Project, Initial Reports 73,* 725–735. Washington DC: U. S. Government Printing Office.

PREMOLI SILVA, I., COCCIONI, R. and MONTANARI, A., Eds., 1988. *The Eocene–Oligocene boundary in the Marche–Umbria Basin (Italy)*. Ancona: Fratelli Anniballi. International Union of Geological Sciences International Subcommission on Paleogene Stratigraphy, Special Publication, 268 pp.

PROTO DECIMA, F., ROTH, P. H. and TODESCO, L., 1975. Nannoplancton calcareo del Paleocene e dell'Eocene della sezione di Possagno. In: Bolli, H. M., Ed., *Monografia micropaleontologica sul Paleocene e l'Eocene di Possagno, Provincia di Treviso, Italia,* 35–55. Solothurn: Schweizerische Palaeontologisches Gesellschaft.

RIO, D., RAFFI, I. and VILLA, G., 1990. Pliocene–Pleistocene calcareous nannofossil distribution patterns in the western Mediterranean. In: Kastens, K.A., Mascle, J., et al., *Proceedings of the Ocean Drilling Program, Scientific Results*, *107,* 513–533. College Station, TX: Ocean Drilling Program.

ROBERTSON, A. H. F., EMEIS, K.-C., RICHTER, C. and CAMERLENGHI, A., et al., 1998 *Proceedings of the Ocean Drilling Program, Scientific Results*, *160*. College Station, TX: Ocean Drilling Program.

ROTH, P. H., 1983. Jurassic and Lower Cretaceous calcareous nannofossils in the western North Atlantic (Site 534): biostratigraphy, preservation, and some observations on biogeography and paleoceanography. In: Sheridan, R. E., Gradstein, F. M., et al., *Deep Sea Drilling Project, Initial Reports 76,* 587–621. Washington DC: U. S. Government Prtinting Office.

ROTH, P. H. and THIERSTEIN, H. R., 1972. Calcareous nannoplankton: Leg XIV of the Deep Sea Drilling Project. In: Hayes, D. E. and Pimm, A. C., et al., *Deep Sea Drilling Project, Initial Reports 14,* 421–486. Washington DC: U. S. Government Prtinting Office.

SEXTON, P. F., NORRIS, R. D., WILSON, P. A., PÄLIKE, H., WESTERHOLD, T., RÖHL, U. BOLTON, C. T. and GIBBS, S., 2011. Eocene global warming events driven by ventilation of oceanic dissolved organic carbon. *Nature*, 471: 349–352.

SEXTON, P. F., WILSON, P. A. and NORRIS, R. D., 2006. Testing the Cenozoic multisite composite $\delta^{18}O$ and $\delta^{13}C$ curves: New monospecific Eocene records from a single locality, Demerara Rise (Ocean Drilling Program Leg 207). *Paleoceanography,* 21: PA2019.

TOFFANIN, F., AGNINI, C., FORNACIARI, E., RIO, D., GIUSBERTI, L., LUCIANI, V., SPOFFORTH, D. J. A. and PÄLIKE, H., 2011. Changes in calcareous nannofossil assemblages during the Middle Eocene Climatic Optimum: Clues from the central–western Tethys (Alano section, NE Italy). *Marine Micropaleontology*, 81: 22–31.

TRIPATI, A. and ELDERFIELD, H., 2005a. Deep-sea temperature and circulation changes at the Paleocene–Eocene thermal maximum. *Science*, 308: 1894–1898.

VILLA, G., FIORONI, C., PEA, L., BOHATY, S. M. and PERSICO, D., 2008. Middle Eocene– late Oligocene climate variability: Calcareous nannofossil response at Kerguelen Plateau, Site 748. *Marine Micropaleontology,* 69: 173–192.

WADE, B. S., 2004. Planktonic foraminiferal biostratigraphy and mechanisms in the extinction of Morozovella in the late middle Eocene. *Marine Micropaleontology,* 51: 23–38.

WEI, W. and THIERSTEIN, H. R., 1991. Upper Cretaceous and Cenozoic calcareous nannofossils of the Kerguelen Plateau (southern Indian Ocean) and Prydz Bay (East Antarctica). In Barrow, B., Larsen, B., et al., *Proceedings of the Ocean Drilling Program, Scientific Results*, *119*, 467– 492. College Station, TX: Ocean Drilling Program.

WEI, W. and WISE JR., S. W., 1989. Paleogene calcareous nannofossil magnetobiostratigraphy: results from South Atlantic DSDP 516. *Marine Micropaleontology,* 14: 119–152.

———, 1990. Biogeographic gradients of middle Eocene–Oligocene calcareous nannoplankton in the South Atlantic Ocean. *Palaeogeoraphy, Palaeoclimatology, Palaeoecoogy,* 79: 29– 61.

———, 1992. Oligocene–Pleistocene calcareous nannofossils from Southern Ocean Sites 747, 748, and 751. In Wise, S. W., Jr., Schlich, R., et al., *Proceedings of the Ocean Drilling Program, Scientific Results*, *120,* 509–521, College Station, TX: Ocean Drilling Program

WESTERHOLD, T. and RÖHL, U., 2009. High resolution cyclostratigraphy of the early Eocene – new insights into the origin of the Cenozoic cooling trend. *Climate of the Past,* 3: 309–327.

WESTERHOLD, T., RÖHL, U., WILKENS, R., et al.,, 2012. Revised composite depth scales and integration of IODP Sites U1331–U1334 and ODP Sites 1218–1220. In Pälike, H., Lyle, M., Nishi, H., et al., *Pacific equatorial transect,* 1–137. Tokyo: Integrated Ocean Drilling Program Management International, Inc. IODP Proceedings, 320/321

ZACHOS, J. C., BREZA, J. and WISE, S. W., 1992. Early Oligocene ice–sheet expansionon Antartica: sedimentological and isotopic evidence from Kerguelen Plateau. *Geology*, 20: 569–573.

ZACHOS, J. C., PAGANI, M., SLOAN, L., THOMAS and E., BILLUPS, K., 2001. Trends, rhythms, and aberrations in global climate 65 Ma to present. *Science*, 292: 686–693.

ZACHOS, J. C., DICKENS, G. R. and ZEEBE, R. E., 2008. An early Cenozoic perspective on greenhouse warming and carbon–cycle dynamics. *Nature*, 451: 279–283.

Received October 8, 2012
Accepted April 18, 2013
Published September 18, 2013